无 机 化 学 学 报

2015 年　　第 31 卷　　第 11 期

目　次

论　文

CHINESE JOURNAL OF INORGANIC CHEMISTRY

Vol.31 No.11 Nov. 2015

CONTENTS

Cover

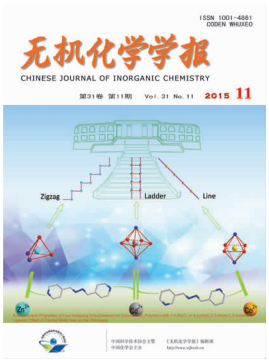

Assembly and Properties of Four Intriguing One-Dimensional Coordination Polymers with 1,4-Bis(3- or 4-pyridyl)-2,3-diaza-1,3-butadiene Ligands: Effect of Central Metal Ions on the Structures (English)

ZHOU Jie, DONG Shun-Fang, QIAO Yong-Feng, DU Lin, YAN Tong, XIE Ming-Jin, ZHAO Qi-Hua

DOI:10.11862/CJIC.2015.294

Chinese J. Inorg. Chem., **2015**,**31**:2095-2102

Articles

Assembly and Properties of Four Intriguing One-Dimensional Coordination Polymers with 1,4-Bis(3- or 4-pyridyl)-2,3-diaza-1,3-butadiene Ligands: Effect of Central Metal Ions on the Structures (English)

ZHOU Jie, DONG Shun-Fang, QIAO Yong-Feng, DU Lin, YAN Tong, XIE Ming-Jin, ZHAO Qi-Hua

DOI:10.11862/CJIC.2015.294

Chinese J. Inorg. Chem., **2015**,**31**:2095-2102

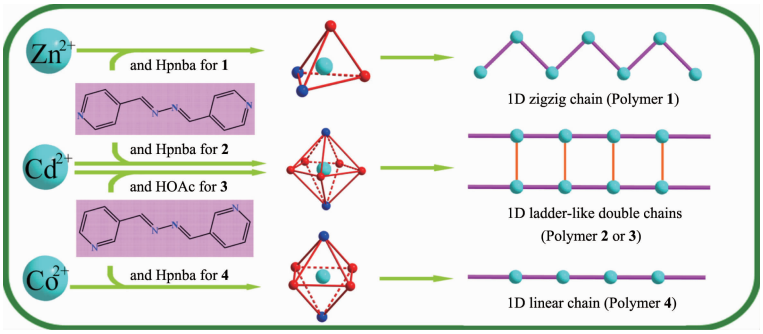

Four one-dimensional coordination polymers show the effect of central metal ions on the structures.

A Microporous 3D MOF Constructed from An Acylamide Tetracid Ligand: Effective Reversible Iodine Adsorption Property (English)

HANG Cheng, LU Zhi-Yong, MENG Fei, JIANG Jing-Jing, BAI Jun-Feng

DOI:10.11862/CJIC.2015.276

Chinese J. Inorg. Chem., **2015**,**31**:2103-2110

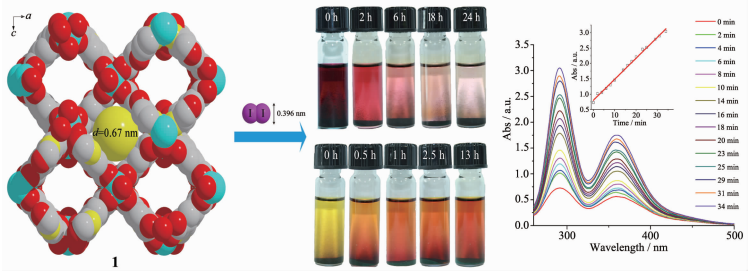

One metal-organic framework with regular porosity constructed from one acylamide tetracid ligand and copper ions exhibits an outstanding performance in reversible adsorption of iodine molecules.

Two Different Co(Ⅱ) Interpenetrating Networks Based on a Flexible Dicarboxylic Acid and Different Bis(imidazole) Ligands (English)

YANG Yu-Ting, TU Chang-Zheng,
MIAO Jiao-Jiao, LI Jun-Li, CHEN Guang

DOI:10.11862/CJIC.2015.291
Chinese J. Inorg. Chem., **2015**,**31**:2111-2118

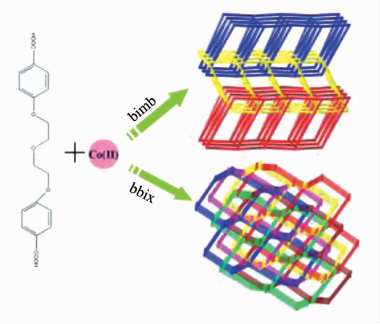

Complex **1** displays 2D→3D 3-fold interpenetrating framework with 4-connected **sql** topology; complex **2** shows a 3D 4-connected framework of 6^6 **dia** topology with 6-fold interpenetration. The magnetic properties of the two complexes indicate typical antiferromagnetic interactions.

Effect of Alkaline Concentration on Mesopore Formation in Acid Pre-treated HZSM-5 Zeolite and Its Catalytic Performance in the Methanol-to-Gasoline Reaction

CHANG Jiang-Wei, FU Ting-Jun,
ZHANG Hong-Jian, ZHOU Hao, LI Zhong

DOI:10.11862/CJIC.2015.278
Chinese J. Inorg. Chem., **2015**,**31**:2119-2127

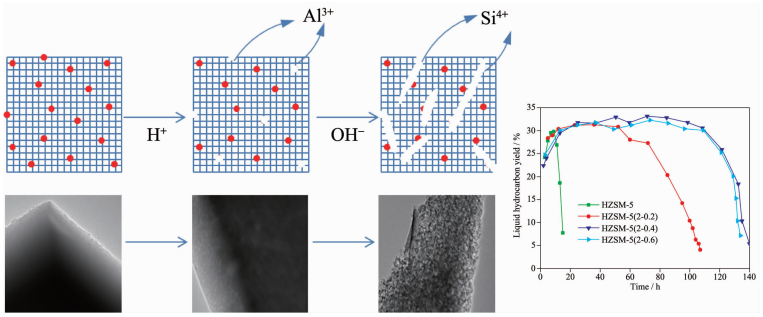

For ZSM-5 zeolite, the acid pre-treatment could facilitate formation of mesoporous structure in alkaline treatment process. With the increase of alkaline treatment intensity, the mesopore structure was increased and the strong acidity was decreased, which resulted in high catalytic activity and long lifetime for MTG reaction.

Preparation and Electrochemical Capacitance Profile of Carrot-Based Porous Carbon

ZHONG Jia-Liang,
GUO Feng-Jiao, MI Hong-Yu

DOI:10.11862/CJIC.2015.299
Chinese J. Inorg. Chem., **2015**,**31**:2128-2134

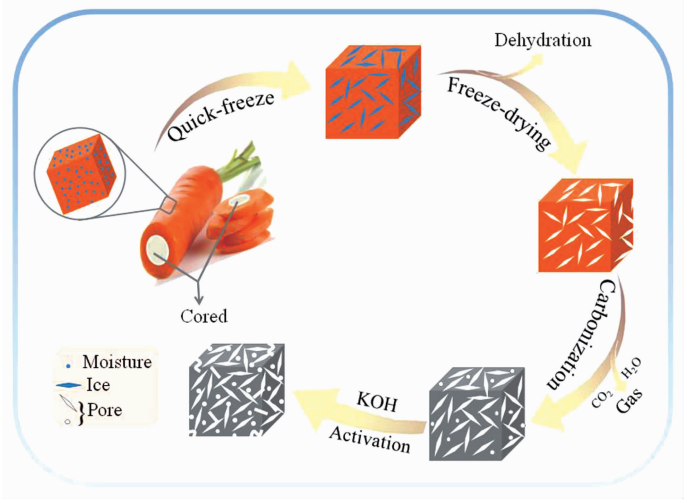

Effects of Metals and Dielectrics on the Optical Absorption Properties of Metal Nano-Particles Dispersed Composite Films

ZHANG Su-Wei, ZHANG Bo-Ping, LI Shun,
ZHU Li-Feng, ZHANG Yu-Qiao

DOI:10.11862/CJIC.2015.280
Chinese J. Inorg. Chem., **2015**,**31**:2135-2142

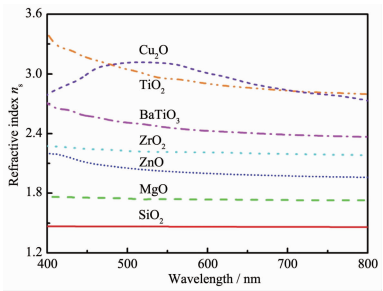

The SPR absorption position in visible region of the composite film is strongly dependent on n_s rather than ε_{m1} and ε_{m2}. The simulated optical absorption spectra of the composite films dispersed by Ag, Au and Cu by Mie theory in this study are in good agreement with the reported experiment results, especially showing a close SPR peak positions to each other.

First-Principles Research on the Electronic and Magnetic Properties of $MgZn_2$ Phase

WANG Hong-Ming, ZHENG Rui, LI Gui-Rong, LI Pei-Si

DOI:10.11862/CJIC.2015.290
Chinese J. Inorg. Chem., **2015**,**31**:2143-2151

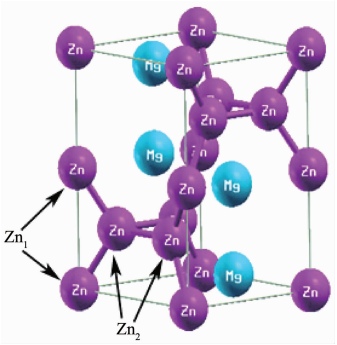

Zn-Mg bond of $MgZn_2$ is generated through interaction of two *sp* hybrid state, which are from Zn4*s*-4*p* hybridized orbit and Mg3*s*-3*p* hybridized orbit separately. $MgZn_2$ phase shows paramagnetism, which stems mainly from the two unpaired electrons in the Zn_1-Mg bond.

Bi_2MoO_6 Hollow Microspheres Preparation and Photocatalytic Properties

ZHANG Qin, WANG Xiao-Feng, DUAN Fang, CHEN Ming-Qing

DOI:10.11862/CJIC.2015.289
Chinese J. Inorg. Chem., **2015**,**31**:2152-2158

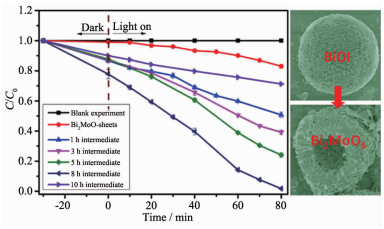

Bi_2MoO_6 photocatalyst with hollow structure was prepared by *in-situ* transformation method using BiOI as self-sacrificing template. The obtained Bi_2MoO_6 hollow microspheres with specific surface area of 61 $m^2 \cdot g^{-1}$ showed higher photocatalytic activity than that of Bi_2MoO_6 sheets or the intermediates obtained at different reaction times.

Syntheses, Crystal Structures, Antioxidant Activity and Quantum Chemistry Calculation of an Acylhydrazone Ligand Containing Thiophene Moiety and Its Cu(Ⅱ) Complex

CHEN Yan-Min, JIANG Xia, CHEN Guang-Hui, XIE Qing-Fan

DOI:10.11862/CJIC.2015.285
Chinese J. Inorg. Chem., **2015**,**31**:2159-2166

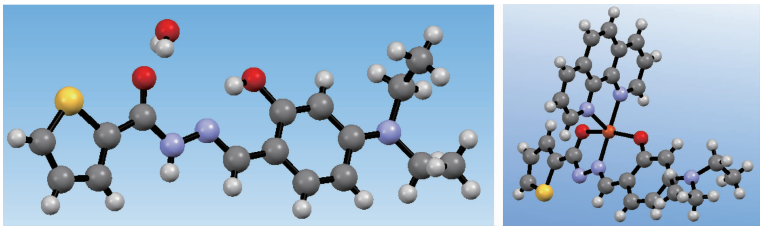

A designed acylhydrazone-type Schiff base ligand H_2L containing sulfur, derived from the condensation of 4-(diethylamino)salicylaldehyde and thiophene-2-formylhydrazine, reacts with Cu(Ⅱ) acetate and phen yielded a complex [Cu(Phen)L].

Photocatalytic Water Splitting for Hydrogen Evolution over CuO/TiO_2 with Ethylene Glycol as Electron Donor

YANG Xu, LI Xiao-Long, HU Cai-Hua, SHA Zuo-Liang, YANG Li-Bin

DOI:10.11862/CJIC.2015.234
Chinese J. Inorg. Chem., **2015**,**31**:2167-2173

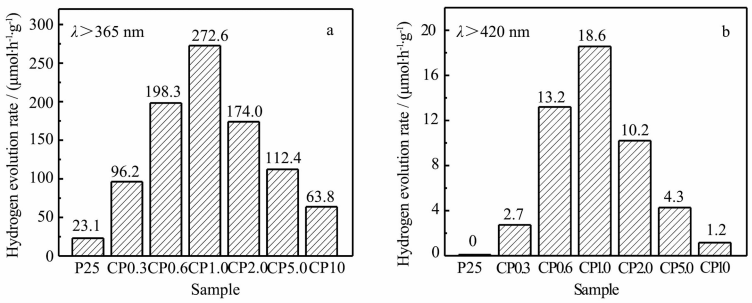

The effect of CuO loading on the reaction rate of photocatalytic hydrogen evolution was studied, by using UV-Visible light (a) and visible light (b) under irradiation of 300 W xenon lamp.

Porous TiO_2 Film with Scaffold Structure for Enhanced Photovoltaic Performance of Dye-Sensitized Solar Cells

HE Feng-Long, WANG Ping, HUANG Yan-Min

DOI:10.11862/CJIC.2015.298
Chinese J. Inorg. Chem., **2015**,**31**:2174-2180

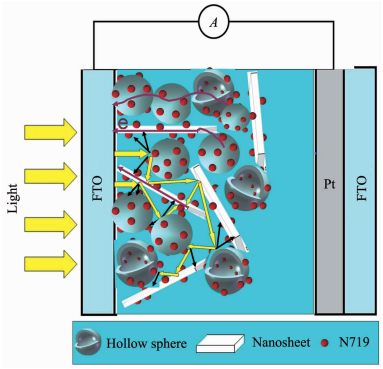

The photoanode of DSSC has an ingenious structures which combine the TiO_2 hollow spheres as the main substrate with the TiO_2 nanosheets as the scaffold. Compared with nonporous TiO_2 film and no scaffold TiO_2 film in DSSC, the porous TiO_2 film with this superior structure have the highest efficiency and performance, which attribute to TiO_2 nanosheets as the scaffold for enhancing the light scattering and TiO_2 hollow spheres as the main substrate for providing more active dye adsorption sites.

Preparation and Properties of Nickel Substituted Cobalt Ferrite Hollow Microspheres

DUAN Hong-Zhen, CHEN Guo-Hong,
ZHOU Fang-Ling, LI Qiao-Ling,
ZHAO Li-Ping

DOI:10.11862/CJIC.2015.296
Chinese J. Inorg. Chem., **2015**,**31**:2181-2187

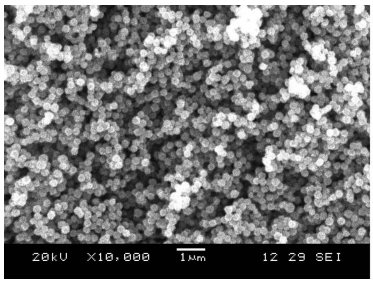

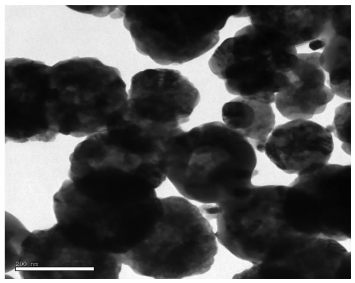

The nano nickel substituted cobalt ferrite hollow microspheres with uniform particle size and good dispersion were prepared by solvent thermal method. The average particle size is about 200 nm.

Synthesis and Antitumor Activity of Dinuclear Platinum Complexes with ($1^{i}R$,$1^{ii}R$,$2^{i}R$,$2^{ii}R$)-N^{i},N^{ii}-(1,3-Phenylenebis(methylene))dicyclohexane-1,2-diamie as the Ligand

GAO Chuan-Zhu, CHEN Ji,
WANG Tian-Shuai, ZHANG Yan,
QIAN Yun-Xu, YANG Bo, GOU Shao-Hua,
DONG Peng, ZHANG Ying-Jie

DOI:10.11862/CJIC.2015.277
Chinese J. Inorg. Chem., **2015**,**31**:2188-2196

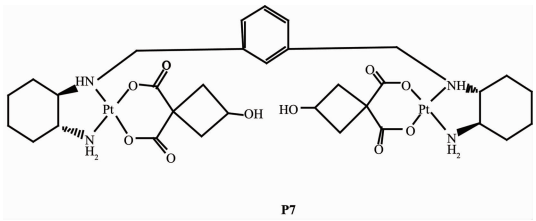

Seven dinuclear platinum (Ⅱ) compounds with a chiral ligand were designed, prepared and biological evaluated. Among them, compound **P7**, owing to 3-hydroxycyclobutane-1,1-dicarboxylate as the leaving group, gave better antitumor activity than carboplatin against HepG-2 and A549 cell lines, and close cytotoxicity to oxaliplatin against HCT-116 cell line. It will be a promising leading compound for further biological evaluations.

Visible-Light Photocatalytic Properties of $Ti_{1-x}V_xO_2$ Films with Dominant {211} Facets Deposited at Room Temperature

XIE Peng-Cheng, HUANG Jie

DOI:10.11862/CJIC.2015.279
Chinese J. Inorg. Chem., **2015**,**31**:2197-2204

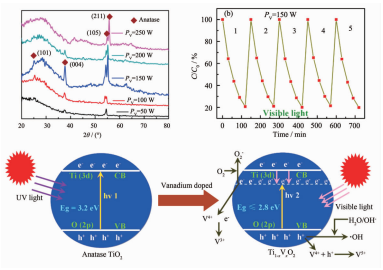

The optical absorption edge of the $Ti_{1-x}V_xO_2$ films shifted towards visible-light zone, improving the visible-light photocatalytic properties of the films. Meanwhile, high energy facet {211} helped to enhance photocatalytic activities of the films to a certain extent.

Preparation and Crystal Structures of Cobalt and Nickel Complexes Containing a Pyridine-Amine Polydentate Ligand

SHI Wei-Dong, ZHENG De-Hua, WANG Mei

DOI:10.11862/CJIC.2015.297
Chinese J. Inorg. Chem., **2015**,**31**:2205-2212

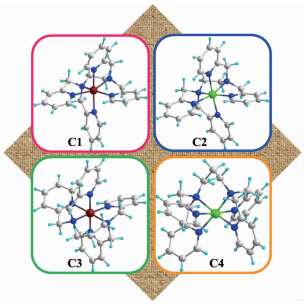

Four cobalt /nickel complexes containing a pyridine-amine ligand were prepared and characterized. The X-ray single crystal diffraction analysis shows that the complexes all belong to the monoclinic crystal system but with different space groups and distinct three-dimensional packing structures.

Anion-Controlled Assembly of Ag(I) Coordination Polymers Based on *trans*-Bis(benzoylacetone)-1, 4-cyclohexanediimine Ligands: Syntheses, Structures, and Solid State Luminescence

ZHANG Qi-Long

DOI:10.11862/CJIC.2015.295
Chinese J. Inorg. Chem., **2015**,**31**:2213-2220

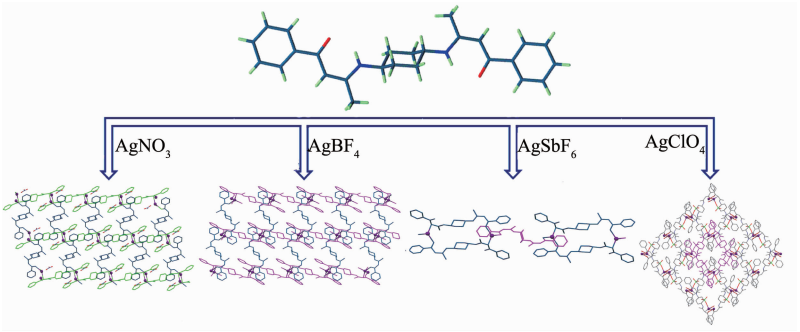

Structural Diversity of Two Cadmium(Ⅱ) Polymers Based on Pyrazine Derivative Ligand: Syntheses, Crystal Structures and Bioactivities (English)

WANG Cui-Juan, MAO Kai-Li, DAI Hai-Yu, LIU Xiao-Lei, MENG Tao, ZHANG Zhi-Bin, ZHOU Xian-Li, WANG Yao-Yu

DOI:10.11862/CJIC.2015.267
Chinese J. Inorg. Chem., **2015**,**31**:2221-2228

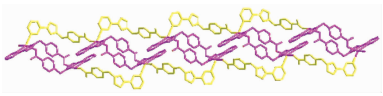

Under same conditions, ligand derived from Pyrazine was selected and reacted with different Cadmium(Ⅱ) salts, producing two coordination compounds $[Cd(L)_2]_n$ (**1**), $[Cd_2(L)_2(CH_3COO)_2(H_2O)_2]$ (**2**) (HL =4-((3-(pyrazin-2-yl)-1*H*-pyrazol-1-yl)methyl) benzoic acid) , which were characterized by element analysis, TGA, fluorescence spectrum and single X-ray crystal diffraction. Structural discrepancy in compounds **1** and **2** can be assigned to different chelating modes of carboxylate groups of ligand, as well as ions effect.

Luteolin and Luteolin-Cr(Ⅲ) Complexes: Antioxidation and Reaction Mechanism with Hydrogen Peroxide Radical (English)

GAO Li-Guo, SONG Xiao-Li, CAO Wei, LÜ Ling-Ling

DOI:10.11862/CJIC.2015.275
Chinese J. Inorg. Chem., **2015**,**31**:2229-2235

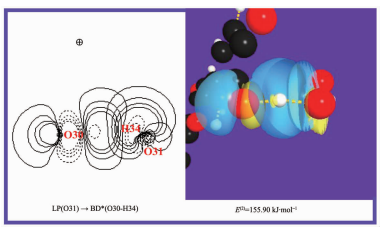

The breakage of O30-H34 bond can be attributed to the transfer of electron density from LP(O31) to anti-bonding BD*(O30-H34). Thus, the orbital interaction leads to the weakening of the O30-H34 bond. The large $E^{(2)}$ value shows a strong orbital interaction.

Five Transition Metal Complexes with 5-Hydroxy-pyridine-2-carboxylic Acid: Syntheses, Crystal Structures and Luminescence Properties (English)

GAO Peng, BING Ying-Ying, ZHANG Ling-Ling, HU Ming

DOI:10.11862/CJIC.2015.287
Chinese J. Inorg. Chem., **2015**,**31**:2236-2242

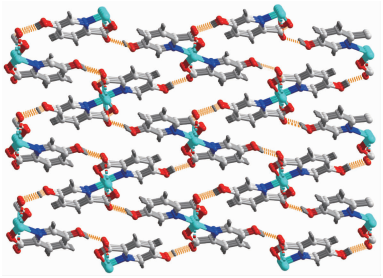

Five mononuclear transition metal compounds based on 5-hydroxy-pyridine-2-carboxylic acid have been obtained, which exhibit the different three-dimensional supramolecular architectures by strong hydrogen-bonding interactions.

Syntheses and Structural Characterization of Copper Complexes with Thioether-Containing Pyridylalkylamide Ligands (English)

WANG Zhao-Dong

DOI:10.11862/CJIC.2015.283
Chinese J. Inorg. Chem., **2015**,**31**:2243-2248

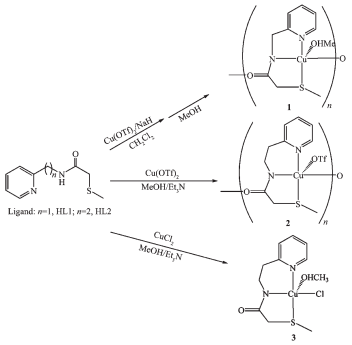

Two one-dimensional copper coordination polymers and one mononuclear copper complex based on thioether-containing pyridylalkylamide ligands have been prepared. Their different coordination modes of the copper center are assigned as the influence of the coordinated ligand.

Syntheses, Crystal Structures and Antitumor Activities of Three Ln(Ⅲ) Complexes with 2-Acetylpyridine Picolinohydrazone (English)

XU Zhou-Qing, MAO Xian-Jie, ZHANG Xin, CAI Hong-Xin, BIE Hong-Yan, XU Jun, JIA Lei

DOI:10.11862/CJIC.2015.281
Chinese J. Inorg. Chem., **2015**,**31**:2249-2256

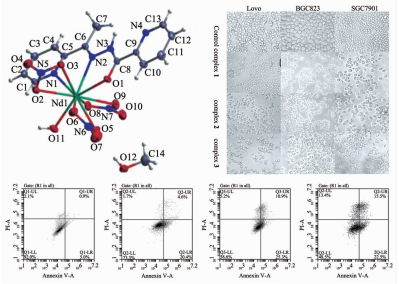

Three Ln(Ⅲ) complexes based on acylhydrazone ligands have excellent antitumor activity towards Lovo human colorectal cancer, BGC823 and SGC7901 human gastric cancer cell lines.

Photoelectrode of Polyanilines/n-Si(111) Crystalline: Preparation and Photoelectric Property

Loteia El Majdoub, LI Jun, ZHANG Yue-Juan, LI Ni-Li, XU Qing-Hong

DOI:10.11862/CJIC.2015.282
Chinese J. Inorg. Chem., **2015**,**31**:2257-2264

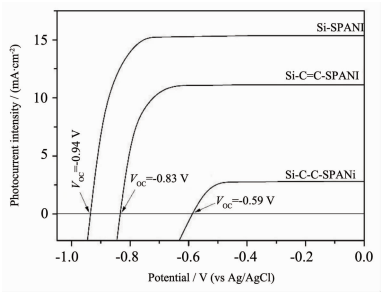

A strong photoelectric conversion rule was found in electrodes based on polyanilines with different substituted groups grafted on n-Si (111) crystalline surface, and a high photocurrent density of 15.4 mA · cm^{-2} and photoelectric transformation efficiency of 13.3% was obtained.

Two Cadmium(Ⅱ) Complexes of an Acylhydrazone Ligand Bearing Quinoline Unit: Syntheses, Structures and Fluorescent Properties (Englsih)

LI Xiao-Jing, WU Wei-Na, XU Zhou-Qing, LI Shou-Jie, ZHAO Liang

DOI:10.11862/CJIC.2015.303
Chinese J. Inorg. Chem., **2015**,**31**:2265-2271

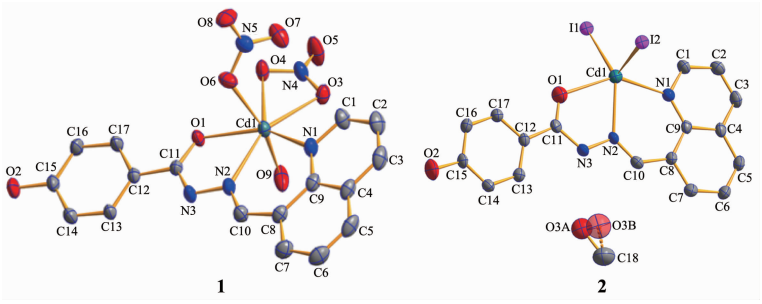

Syntheses, Crystal Structures and Fluorescent Properties of Two Coordination Polymers Based on 4,4′-Bis(imidazol-l-yl)diphenyl Thioether and Phthalic Acid (English)

XU Han, ZHENG He-Gen

DOI:10.11862/CJIC.2015.284
Chinese J. Inorg. Chem., **2015**,**31**:2272-2278

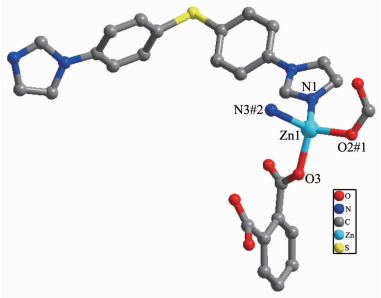

Two coordination polymers have been synthesized and characterized by elemental analyses, IR spectra, TGA and the crystal structures were determined by single-crystal X-ray diffraction. The thermal stability and solid-state photoluminescences of compounds **1** ~**2** were explored.